Borrell Tomás, MA.; Torrecillas, R.; Rocha, VG.; Fernandez, A.; Bonache Bezares, V.; Salvador Moya, MD. (2012). Effect of CNFs content on the tribological behaviour of spark plasma sintering ceramic-CNFs composites. Wear. 274:94-99. doi:10.1016/j.wear.2011.08.013.

Effect of CNFs content on the tribological behaviour of spark plasma sintering ceramic-CNFs composites

A. Borrell[1*], R. Torrecillas[1], V.G Rocha[2], A. Fernández[2], V. Bonache[3], M.D. Salvador[3]

[1]Centro de Investigación en Nanomateriales y Nanotecnología (CINN) (Consejo Superior de Investigaciones Científicas - Universidad de Oviedo - Principado de Asturias), Parque Tecnológico de Asturias, 33428 Llanera (Asturias), Spain

[2]ITMA Materials Technology, Parque Tecnológico de Asturias, 33428 Llanera (Asturias), Spain

[3]Instituto de Tecnología de Materiales (ITM), Universidad Politécnica de Valencia, Camino de Vera, s/n, 46022 Valencia, Spain

*Corresponding author. Address: *Centro de Investigación en Nanomateriales y Nanotecnología (CINN), Parque Tecnológico de Asturias, 33428 Llanera (Asturias), Spain*. Tel.: +34 985 980 058; Fax: +34 985 265 574

E-mail address: a.borrell@cinn.es (A. Borrell)

ABSTRACT

Alumina-carbon nanofibres (CNFs) and silicon carbide-CNFs nanocomposites with different volume fraction of CNFs (0-100 vol.%) were obtained by spark plasma sintering. The effect of CNFs content on the tribological behaviour in dry sliding conditions on the ceramic-carbon nanocomposites has been investigated using the ball-on-disk technique against alumina balls. The wear rate of ceramic-CNFs nanocomposites decreases with CNFs increasing content. The friction coefficient of the

Al_2O_3/CNFs and SiC/CNFs nanocomposites with high CNFs content was found to be significantly lower compared to monolithic Al_2O_3 and SiC due to the effect of CNFs and unexpectedly slightly lower than CNFs material. The main wear mechanism in the nanocomposite was abrasion of the ceramic and carbon components which act in the interface as a sort of lubricating media. The experimental results demonstrate that the addition of CNFs to the ceramic composites significantly reduces friction coefficient and wear rate, resulting in suitable materials for unlubricated tribological applications.

Keywords: Ceramic-matrix composite; Wear; Carbon nanofibres; Tribology; Hardness

1. INTRODUCTION

The continuous improvement of the carbon nanofibres (CNFs) and carbon nanotubes (CNTs) production techniques and thus the available qualities of these materials, have promoted their introduction into polymers [1,2], ceramics [3-5] and metals [6-8] matrices. In recent years some research studies have demonstrated the positive effect of CNFs in alumina-, zirconia- and silicon carbide-based composites [9-13]. Maensiri et al. [9] reported an improvement of approximately 13% in the fracture toughness of alumina-CNFs composites with 2.5 vol.% CNFs, but the hardness and fracture strength decreases with increasing volume fraction of CNFs. Duszová et al. [10] using similar CNFs contents found that the zirconia-CNFs composites exhibit slightly higher mechanical properties. Although the ceramic-CNFs nanocomposites firstly developed were focused on low CNFs content (usually <10 vol.%), Borrell et al. [12] have already studied CNFs/Al_2O_3 nanocomposites with high CNFs content (50-100) vol.%. They reported that carbon matrix components with a mechanical improvement of 60% in

relation with pure carbon materials can be achieved by 50 vol.% Al_2O_3 addition. This kind of nanocomposites can be obtained thanks to the relatively low sintering temperature used during Spark Plasma Sintering (SPS) technique. They have also demonstrated that an interface improvement between Al_2O_3 and CNFs by a surface coating with alumina precursor improves mechanical properties of the composites with high CNFs content (90 vol.%). Shimoda et al. [13] studied the hot-pressing of CNFs/SiC nanocomposites with 1-10 wt.% of CNFs via a transient eutectic phase route at 1900 ºC for 1h, using Al_2O_3 and Y_2O_3 particles as sintering additives. They achieved well dispersed CNFs on the nanocomposite with contents below 5 wt.% and reached 98 % relative density on the CNFs/SiC composites.

Ceramics are potential materials to be used in friction systems. They offer high values of specific heat and medium (Al_2O_3) to high (SiC) values of thermal conductivity as well as high oxidation and thermal resistance. In addition to their functional properties, the research on ceramic-CNTs or ceramic-CNFs composites has been focused on their basic mechanical properties such as hardness, strength and fracture toughness, electrical conductivity and only limited work on their tribological behaviour has been attempted [14-17]. In these studies it was observed that the friction coefficient was reduced by the addition of CNTs to the ceramic matrix. Lim et al. [16] investigated the tribological behaviour of alumina/CNTs composites with different weight contents of CNTs (0-12 wt.%) fabricated by hot-pressing and tape casting, followed by lamination and hot-pressing. They reported that the tape-casting process significantly improves the uniform distribution of CNTs in the alumina matrix, resulting in an enhanced wear resistance of the composites. Ahmad et al. [17] investigated the effect of MWCNTs addition in coefficient of friction and wear resistance of hot-pressed alumina-MWCNTs nanocomposites (reinforced with 2, 5 and 10 wt.% MWCNTs). They found reduced

coefficients of friction and improved wear resistance for the nanocomposites obtained at low and moderate sliding loads; whilst for high sliding loads (35 N), the 10 wt.% MWCNT nanocomposite exhibited lower wear resistance. Wang et al. [18] reported that the addition of silicon carbide (SiC) to the matrix of C/C composites improves their tribological properties, by combining the hardness and the chemical stability of SiC with the self-lubricating action of carbon. Hvizdos et al. [19] studied the tribological behaviour of CNFs-zirconia composites sintered by hot-pressing. They demonstrated an excellent frictional properties of ZrO_2/CNFs can be achieved by incorporating a low amount (1.07 wt.%) of CNTs into the microstructure of zirconia. The friction coefficient of ZrO_2/CNFs composite was found to be significantly lower compared to that for monolithic zirconia with relatively low wear rates for both materials.

The present work aims to study the tribological behaviour of ceramic-CNFs nanocomposites sintered by Spark Plasma Sintering technique either at high and low CNFs content and without additional sintering additives. Then, ceramic reinforced carbon materials and CNFs reinforced ceramic materials were investigated. Al_2O_3/xCNFs and SiC/xCNFs (x=0-100 vol.%) nanocomposites have been prepared and the role of ceramic-CNFs debris of the composites on the frictional coefficient and wear rate have been investigated.

2. EXPERIMENTAL PROCEDURE

The materials used in this study were commercial carbon nanofibres (CNFs) having an average outer diameter of 20-80 nm and lengths >30 μm, supplied by Group Antolín Engineering, (Burgos, Spain). These stacked-cup CNFs were generated via vapour phase growth (VGCNFs) [20] using natural gas as a carbon feedstock, a Ni compound

as catalyst (6-8%), hydrogen and a sulphur source at temperatures above 1100 ºC. It is highly graphitic with no presence of amorphous carbon coating. This sample has been deeply characterized elsewhere [21]. α-Al_2O_3 nanopowder (Taimei TM-DAR Chemicals Co. Ltd, Japan) with an average particle size of 153 nm and a purity of 99.99% was used as one of the ceramic systems. β-SiC nano-sized powder (Hubei Minmetals Corp., China) with a mean particle diameter of 50 nm and a purity >98% was used as the second ceramic material. The powder mixtures, Al_2O_3/CNFs = 100/0 - 80/20 - 50/50 - 20/80 - 0/100 vol.% and SiC/CNFs = 100/0 - 80/20 - 50/50 - 20/80 - 0/100 vol.%, were dispersed in ethanol (Panreac Quimica) by high-energy attrition milling (Union Process, EE.UU) using alumina balls of 2 mm diameter at 400 rpm and milling times of 1 hour. After milling, the resulting slurry was dried at 60 ºC and the dried powder was sieved under 60 μm. The powder samples were placed into a graphite die with an inner diameter of 20 mm and cold uniaxially pressed at 30 MPa. Then, they were introduced in a spark plasma sintering apparatus HP D 25/1 (FCT Systeme GmbH, Rauenstein, Germany) under low vacuum (10^{-1} mbar). It was applied 80 MPa of uniaxial pressure and a heating rate of 100 ºC min^{-1} was used. The composites of Al_2O_3/CNFs and SiC/CNFs were sintered at 1500 ºC and 1600 ºC, respectively. In the case of SiC/CNFs materials, no sintering additives were used. Bulk density of the sintered bodies was measured by the geometric method from weight and geometric volume of the material. Relative densities were calculated as the relation between geometrical and theoretical densities. These theoretical densities were calculated by the rule of mixtures using 2.00 g cm^{-3}, 3.21 g cm^{-3} and 3.98 g cm^{-3} as densities for carbon nanofibres, silicon carbide and alumina, respectively. Raman spectra were obtained by Raman spectrometer XY modular (Dilor) with a CCD4 detector. The excitation source used was an argon laser, model Specra-Physics 265, which used the green line

wavelength of 532 nm. The laser power used was 20 mW and the slit width of 200 microns. The spectra obtained were deconvoluted to separate the peaks by adjusting the rate curves Lorentzian/Gaussian for calculating the parameters. The position and width of the bands were used to estimate the degree of order of the materials. The degree of disorder was estimated from the relationship I_D/I_T, where I_D corresponds to the intensity of D band (1350 cm^{-1}) and I_T corresponds to the total intensity of all first-order bands (D, G, D´ at 1350, 1580 and 1620 cm^{-1}, respectively).

The samples for hardness analysis were previously polished (Struers, model RotoPol-31) with diamond to 1 μm roughness. The hardness of the materials was determined using the indentation technique (Buehler, model Micromet 5103) with a conventional diamond pyramid indenter. The diagonals of each indentation were measured using an optical microscope. Measuring conditions for the Vickers hardness, H_v, were an applying load of 2 N for 10 s and the standard specification ASTM E92-72. The value of H_v is the relationship between applied load P and the surface area of the diagonals of indentation [22]. Wear tests were carried out under dry sliding conditions using a tribometer ball-on-disk according to ASTM wear testing standard G99-03. As friction partners, alumina balls 5 mm in diameter were used. The sample surfaces were polished with 1 micron diamond slurry. The normal load, sliding speed and distance were fixed at 15 N, 250 rpm and 1000 m, respectively. Testing was carried out in air, at room temperature and in dry conditions. The friction coefficient and wear loss were measured and the damage was studied on the worn surfaces of disks using scanning electron microscopy (SEM, Zeiss DSM 950).

3. RESULTS AND DISCUSSION

It is worthwhile to take in account that in the case of ceramic-carbon composites processed by SPS, the integrity of the carbon nanostructures incorporated could be deteriorated due to the high temperature and current density applied. Then, micro-Raman characterization of CNFs materials before and after the sintering process has been previously made. Figure 1 shows the Raman spectra and the calculated parameters of the raw CNFs powder and sintered at 1500 ºC and 2350 ºC. The selection of these temperatures aims to evaluate the transformation of the CNFs at temperatures similar to those commonly used in the processing of ceramic nanocomposites-CNFs (1400-1800 ºC) and on the other hand, subjecting the carbon nanostructured to extreme sintering conditions, as it rarely has been reported in the literature 2350 ºC [23-25].

As it is shown in Figure 1, they are not observed significant changes in the spectrum or calculated parameters of the material sintered at 1500 ºC. Moreover, there is a reduction in the relative intensity of the defective graphitic structures (D-line), when the material is sintered at temperatures above 2350 ºC.

Although some authors have reported negligible damage on carbon nanostructures after SPS process [26-29] there is a big controversy on this topic in the literature. Other researchers [25,30-31] provide solid evidence that the pulsed current promotes damage or the breakdown of the carbon hexagonal unit. Considering the published results and the data shown in this paper, it can be proposed that high temperature behaviour depends on the carbon nanostructures characteristics and therefore, every carbon nanostructure should be profusely characterized in order to know their stability after high temperature treatments.

Figure 2 shows the relative density of the composites and monolithic materials after SPS sintering up to 1500 ºC in the Al_2O_3/CNFs system and 1600 ºC in the SiC/CNFs system.

Two different trends were found depending on the ceramic component studied. In the case of Al_2O_3/CNFs nanocomposites, a decrease in the relative density is observed when the CNFs content is increased. Monolithic alumina sintered by SPS is fully dense (99.9% t.d) while the relative density of bulk CNFs material is around 92.5% t.d. This value is noticeably high for a carbon material obtained at this relatively low temperature (1500 ºC). Although the density of Al_2O_3/20vol.% CNFs nanocomposite is close to theoretical density, for higher CNFs content, the relative density decreases approximately following the rule of mixtures. On the other hand, as it can be appreciated in Figure 2, SiC/CNFs nanocomposites have always lower relative density than bulk CNFs material. It is widely known that the full densification of the SiC ceramics without sintering additives is especially complicated, mainly due to the covalent nature of the silicon carbide bond which in the sintering process shows very low diffusivity of the atoms and high energy on the grain boundaries [32]. The densities achieved for the SiC/CNFs composites sintered by SPS at 1600 ºC clearly show the positive effect of CNFs on SiC densification. While only 75-80% relative density are obtained for SiC/CNFs composites containing up to 50 vol.% CNFs, close to 90% of relative density can be achieved for SiC/80vol.% CNFs at 1600 ºC, even if this temperature can be considered too low for SiC sintering. Taken into account that no other additives were used for assisting SiC densification by liquid phase sintering, this result suggests that carbon nanofibres are acting simultaneously as a second phase for composite designing and as sintering additive themselves, improving the density of the final material.

Hardness values of the monolithic ceramics, bulk CNFs material and Al_2O_3/CNFs and SiC/CNFs composites are summarized in Figure 3. The hardness values of prepared nanocomposites are consistent with major component of the material and its relative

density. Regarding the results obtained for composites of Al_2O_3/CNFs systems, it can be seen how the materials hardness decreases with CNFs content. The soft phase addition as it is carbon nanofibres to obtain ceramic-carbon composites leads to marked reduction in hardness values. The hardness of Al_2O_3/CNFs composite with 20 vol.% CNFs has been reduced at least 27% from monolithic Al_2O_3 material and since the CNFs content is 50 vol.% or higher, the material composites shows a sharp decrease (more than 85% hardness reduction) in the composite in relation with the monolithic alumina reaching values characteristic for carbon materials. In the case of SiC/CNFs composites, similar trend is observed for nanocomposites with CNFs content higher than 50 vol.% but low values are maintained even for monolithic SiC material. The lack of density of this material sintered without sintering additives leads to very low hardness values compared with corresponding to liquid-phase-sintered SiC that are around 25-31 GPa [33].

The evolution of wear rate as a function of CNFs content of the Al_2O_3/CNFs and SiC/CNFs composites and monolithic Al_2O_3, SiC and CNFs material are shown in Figure 4. The wear rate is defined as the wear amount for a unit distance and unit normal load.

Although slightly differences can be found, the logarithmic plot of the obtained wear rate shows that all ceramic-CNFs composites have very similar wear rate independently of the ceramic matrix used and the CNFs content. The only remarkable difference in wear rate corresponds to monolithic ceramic materials, Al_2O_3 and SiC, and it is due to their differences in density, 99.9% and 68.3%, respectively. Full densification of monolithic alumina leads to a noticeably reduction of wear rate whereas the relative

density of monolithic SiC is even lower than corresponding composites, which causes significant mass loss in the SiC test specimen due to the friction of the ball during test.

The slightly decrease of the SiC/CNFs composites wear rate with CNFs content up to 50 vol.% is directly related with the roughness reduction thanks to the density improvement which has been previously shown in Figure 2, combined with the lubricant effect of CNFs. The highest density composite (SiC/CNFs with 80 vol.% of CNFs) shows approximately the same wear rate than SiC/CNFs (50/50) vol.% and slightly lower than bulk CNFs material. These two composites are carbon matrix composites and they show similar wear rate and comparable to corresponding compositions prepared in the Al_2O_3/CNFs system. Considering the manifest difference in relative density for both ceramic/50vol.% CNFs composites, the similar wear rate is due to lubricant effect of carbon matrix which is stronger than roughness caused by lack of density.

The wear rate of Al_2O_3/CNFs composites is higher than monolithic alumina which can be considered negligible. The addition of a soft second phase decreases the hardness of the composite materials as it has been shown in Figure 3. This effect is combined with a reduction in relative density of these composites with CNFs content, from 99.9% to 90.0%, and therefore, an increase in surface roughness. Nevertheless, the wear rate of Al_2O_3/20vol.% CNFs composite is significantly higher than monolithic alumina even though the relative densities are similar. Then, in the case of alumina composites it can be concluded that the loss of hardness has greater influence on the wear rate than relative density.

Figure 5, shows the friction coefficient of Al_2O_3/CNFs and SiC/CNFs composites and monolithic Al_2O_3, SiC and CNFs at an applied load of 15 N in function of CNFs content and distance covered. The friction coefficient of the composites and monolithic materials is nearly constant during the whole test showing only a slightly variation in the first 25 meters of distance Figure 5 (right). In this initial period, there is a grinding due to the elimination of the higher surface roughness followed by tightening of the contact surfaces leading to wear surface layers [34].

The high friction coefficients of Al_2O_3 and SiC monolithic materials (around 0.4-0.6) are typical for ceramic materials [35]. As it can be seen in Figure 5a, the friction coefficient of the nanocomposites decreases when the CNFs content is increased. This is due to the lubricating properties of the CNFs (graphite). The friction coefficient is related with the energy consumption involved in the friction process that is especially high in monolithic ceramics in comparison with ceramic-carbon composites. The rolling motion of CNFs at the interface between the specimen and the ball allows reducing the friction coefficient. A similar lubricating effect was previously reported for multi-walled (MW) CNTs-containing Al_2O_3 composites by An et al. [17] and Yamamoto et al. [14] and for single-walled (SW) CNTs solids by Yamamoto [36]. An et al. reported a 40% decrease in friction coefficient in 12 wt.% MWCNT-Al_2O_3 composite down to the value of 0.3 [17]. Concerning the composites prepared by Yamamoto et al., they reached a minimum friction coefficient (with a value of 0.3) at 4 wt.% of MWCNT content [14].

The monolithic alumina sintered by SPS at 1500 ºC is a full dense ceramic with excellent mechanical properties and therefore, the high friction coefficient is accompanied by low wear rate value as it could be expected. Nevertheless, although monolithic SiC sintered by SPS at 1600 ºC shows similar friction coefficient, its low

relative density is reflected on its considerably higher wear rate. Then, the friction coefficient mainly depends on the type material whereas the wear rate is strongly influenced by materials properties which are consequence of processing parameters. It must be noted the particular behaviour of Al_2O_3/CNFs (80/20) vol.% composite. Its friction coefficient is noticeably high in comparison with all ceramic-carbon nanocomposites. In the literature, even when lower amounts of CNTs or CNFs are added to alumina matrix, a decrease in friction coefficient is observed. In our case, the use of SPS sintering technique allows combining full densification of the material while the alumina grain size is maintained at nanometer scale. As consequence, this composite shows a relative high hardness and its fracture strength (480 MPa) is even higher than monolithic alumina (400 MPa). Then, the material behaviour is more similar to ceramics than carbon materials unlike the other ceramic-carbon nanocomposites. In the case of SiC/CNFs (80/20) vol.% composite, that is not completely dense, the effect of CNFs is stronger and the friction coefficient of the nanocomposite is much lower than corresponding to monolithic SiC.

It must be highlighted that both nanocomposites systems show a minimum in their friction coefficient for compositions with 50 vol.% CNFs. It could be expected that minimum friction coefficient should correspond to bulk CNFs materials, because the carbon content is the responsible of reducing the friction energy involved in the process. However, this minimum in friction coefficient agrees with minimum in wear rate and therefore, it can be concluded that a synergy between the ceramic and CNFs has arisen. The slightly increase in hardness and the roughness reduction due to the addition of low amounts of ceramic phase allows balancing the friction energy involved in the process and the material lost due to wear. These materials are especially attractive to be used in unlubricated tribological applications. When the CNFs is increased from 50 to 80 vol.%,

the friction coefficient slightly increases from an average value of 0.19 to a value of 0.21 for Al_2O_3/CNFs composites and from an average value of 0.17 to 0.22 for SiC/CNFs composites. The value for bulk CNFs material is 0.27. A similar trend is found when the wear rate is compared and this can be related with the reduction of hardness values. For CNFs contents higher than 50 vol.%, the removal of material from sample surface is easier due to the lower mechanical properties of the CNFs material [11], leading to an increase in softer waste that act as a third body. These abrasives form different constituents of wear debris which tended to increase ploughing debris.

SEM micrographs of damaged surfaces after the wear test are shown in Figure 6. The worn surface revealed that the main wear mechanism in the Al_2O_3/CNFs with 20 vol.% of CNFs is self-polishing by low-intensity abrasion and brittle fracture due to the poor cohesion between the CNFs and the matrix. In a previous study on the alumina composites [37], the alumina grains detached from the alumina surface caused abrasion of zirconia material. However, this observation is less significant in our case because of the low applied load. In the worn surface of this material it is possible to observe polished areas and large amount of fine (submicron) wear particles.

The Figure 6a shows the surface covered with pull-out fine alumina grain over the entire worn surface and many cracks. These cracks were observed in the direction of sliding and generated micro-abrasion. CNFs might play an important role in the sliding wear behaviours of ceramics. Several researches have addressed the characterization of the CNFs and their role on the wear behaviours [16-19]. The role of CNFs lubricant formation can drastically reduce the amount of wear in ceramics. The dominant wear behaviour of Al_2O_3/CNFs (20/80) vol.% (Figure 6b) was mild abrasion which resulted in a smooth worn surface.

The main wear behaviour observed in Figure 6 (c) and (d) corresponding to SiC/CNFs composites was cohesive wear. Partial cracks, perpendicular to the sliding direction, were observed during sliding. These cracks are due to the tensile stress at the trailing edge of the contact areas. The surface of SiC/CNFs (80/20) vol.% composite was covered by debris compaction resulted from the frequent events of the micro-fracture due to the lowest densification. Wear debris is a mixture of SiC and CNFs particles.

The CNFs with larger diameter and nanofibres oriented not perpendicularly to the worn surface were ground at applied load, and the resulting graphite together with the crushed CNFs creates the transferred film. It seems that the excellent friction coefficient of the composites is probably related to the smearing of this CNFs film over the contact area, which allows easy shear and then helps to achieve a lubricating effect during sliding [19]. More work is needed to understand the detailed role of CNFs on the tribological performance of these composites.

4. CONCLUSIONS

The results showed how friction and wear behaviour of ceramic/CNF nanocomposite materials are influenced by the type of ceramic component and properties such as hardness or relative density. Superior tribological properties were achieved in two ceramic matrices (Al_2O_3 and SiC) when CNFs are added. The wear rate and the friction coefficients decrease significantly in ceramic-CNFs composites by addition of the CNFs thanks to their lubricating properties and wear debris. However, bulk CNFs material shows a coefficient of friction and wear rate slightly higher than composites with high CNFs content (>50 vol.%) due to its lower hardness. Friction coefficients of ceramic-CNFs composites with 50 vol.% of CNFs were found to be significantly lower than all

materials studied. The carbon-based transferred film over the contact area allows easy shear and helps to create a lubricating effect during sliding. SEM observations showed that dominant wear behaviour of ceramics-CNFs composites were abrasion and brittle fracture.

Acknowledgments

This work has been carried out with financial support of National Plan Projects MAT2006-01783 and MAT2007-30989-E and the Regional Project FICYT PC07-021. A. Borrell, acknowledges the Spanish Ministry of Science and Innovation for her FPI Ph.D. grant. We would like to thank the people from Institute Technological of Materials (ITM) of the Polytechnic University of Valencia for helping us with the tribology experiments during A. Borrell's short stay in 2009.

References

[1] H. Cai, F. Yan, Q, Xue. Investigation of tribological properties of polyimide/carbon nanotube nanocomposites, Mater. Sci. Eng. A 364 (2004) 94-100.

[2] W.X. Chen, F. Li, G. Han, J.B. Xia, L.Y. Wang, J.P. Tu, Z.D. Xu, Tribological Behavior of Carbon Nanotube-Filled. PTFE Composites, Tribol. Lett. 15 (2003) 275-278.

[3] K. Matsui, L.J. Lanticse, Y. Tanabe, E. Yasuda, M. Endo, Stress graphitization of C/C composite reinforced by carbon nanofibers, Carbon 43 (2005) 1577-1579.

[4] G.D. Zhan, J.D. Kuntz, J.L. Wan, A.K. Mukherjee, Single-wall carbon nanotubes as attractive toughening agents in alumina-based nanocomposites, Nat. Mater. 2 (2003) 38-42.

[5] R.W. Siegel, S.K. Chang, B.J. Ash, J. Stone, P.M. Ajayan, R.W. Doremus, L.S. Schadler, Mechanical behavior of polymer and ceramic matrix nanocomposites. Scr. Mater. 44 (2001) 2061-2064.

[6] I.S. Kim, S.K. Lee, Fabrication of carbon nanofiber/Cu composite powder by electroless plating and microstructural evolution during thermal exposure, Scr. Mater. 52 (2005) 1045-1049.

[7] W.X. Chen, J.P. Tu, Z.D. Xu, W.L. Chen, X.B. Zhang, D.H. Cheng, Tribological properties of Ni-P-multi-walled carbon nanotubes electroless composite coating, Mater. Lett. 57 (2003) 1256-1260.

[8] E. Hammel, X. Tang, M. Trampert, T. Schmitt, K. Mauthner, A. Eder, P. Pötschke, Carbon nanofibers for composite applications, Carbon 42 (2004) 1153-1158.

[9] S. Maensiri, P. Laokul, J. Klinkaewnarong, V. Amornkitbamrung, Carbon nanofiber-reinforced alumina nanocomposites: Fabrication and mechanical properties, Mater. Sci. Eng. A 447 (2007) 44-50.

[10] A. Duszová, J. Dusza, K. Tomáseek, J. Morgiel, G. Blugand, J. Kuebler, Zirconia/carbon nanofiber composite, Scr. Mater. 5 (2008) 520-523

[11] A. Borrell, A. Fernández, C. Merino, R. Torrecillas, High density carbon materials obtained at relatively low temperature by spark plasma sintering of carbon nanofibers, Int. J. Mater. Res. 101 (2010) 112-118.

[12] A. Borrell, V.G. Rocha, R. Torrecillas, A. Fernández, Surface coating on carbon nanofibers with alumina precursor by different synthesis routes, Comp. Sci. Technol. 71 (2011) 18-22.

[13] K. Shimoda, T. Hinoki, A. Kohyama, Effect of carbon nanofibers (CNFs) content on thermal and mechanical properties of CNFs/SiC nanocomposites, Comp. Sci. Technol. 70 (2010) 387-392.

[14] G. Yamamoto, M. Omori, K. Yokomizo, T. Hashida, K. Adachi, Structural characterization and frictional properties of carbon nanotube/alumina composites prepared by precursor method, Mater. Sci. Eng. B 148 (2008) 265-269.

[15] Z.H. Xia, J. Lou, W.A. Curtin, A multiscale experiment on the tribological behavior of aligned carbon nanotube/ceramic composites, Scr. Mater. 58 (2008) 223-226.

[16] D.S. Lim, D.H. You, H.J. Choi, S.H. Lim, H. Jang, Effect of CNT distribution on tribological behavior of alumina-CNT composites, Wear 259 (2005) 539-544.

[17] J.W. An, D.H. You, D.S. Lim, Tribological properties of hot-pressed alumina-CNT composites, Wear 255 (2003) 677-681.

[18] Y. Wang, H. Wu, Friction surface evolution of carbon fibre reinforced carbon/silicon carbide (C_f/C-SiC) composites, J. Eur. Ceram. Soc. 30 (2010) 3187-3201.

[19] P. Hvizdos, V. Puchý, A. Duszová, J. Dusza, Tribological behavior of carbon nanofibers-zirconia composite, Scr. Mater. 63 (2010) 254-257.

[20] L. Ci, J. Wei, B. Wei, J. Liang, C. Xu, D. Wu, Carbon nanofibers and single-walled carbon nanotubes prepared by the floating catalyst method, Carbon 39 (2001) 329-335.

[21] J. Vera-Agullo, H. Varela-Rizo, J.A. Conesa, C. Almansa, C. Merino, I. Martin-Gullon, Evidence for growth mechanism and helix-spiral cone structure of stacked-cup carbon nanofibers, Carbon 45 (2007) 2751-2758.

[22] G. Antis, P. Chantikul, B. Lawn, D. Marshall, A Critical Evaluation of Indentation Techniques for Measuring Fracture Toughness: I, Direct Crack Measurements, J. Am. Ceram. Soc. 64 (1981) 533-538.

[23] J. Li, L. Wang, T. He, W. Jiang, Transport properties of hot-pressed bulk carbon nanotubes compacted by spark plasma sintering, Carbon 47 (2009) 1135-1140.

[24] C. Qin, X. Shi, S.Q. Bai, L.D. Chen, L.J. Wang, High temperature electrical and thermal properties of the bulk carbon nanotube prepared by SPS, Mater. Sci. Eng. A. 420 (2006) 208-211.

[25] G. Yamamoto, Y. Sato, T. Takahashi, M. Omori, T. Hashida, A. Okubo, K. Tohji, Single-walled carbon nanotube-derived novel structural material, J. Mater. Res. 21 (2006) 1537-1542.

[26] M. Mazaheri, D. Mari, R. Schaller, G. Bonnefont, G. Fantozzi, Processing of yttria stabilized zirconia reinforced with multi-walled carbon nanotubes with attractive mechanical properties, J. Eur. Ceram. Soc. Article in Press, doi:10.1016/j.jeurceramsoc.2010.11.009

[27] S.R. Bakshi, V. Musaramthota, D.A. Virzi, A.K. Keshri, D. Lahiri, V. Singh, S. Seal, A. Agarwal, Spark plasma sintered tantalum carbide–carbon nanotube composite: Effect of pressure, carbon nanotube length and dispersion technique on microstructure and mechanical properties, Mater. Sci. Eng. A 528 (2011) 2538-2547.

[28] H. Kwon, M. Estili, K. Takagi, T. Miyazaki, A. Kawasaki, Combination of hot extrusion and spark plasma sintering for producing carbon nanotube reinforced aluminum matrix composites, Carbon 47 (2009) 570-577.

[29] X. Wang, N.P. Padture, H. Tanaka, Contact-damage-resistant ceramic/single-wall carbon nanotubes and ceramic/graphite composites, Nat. Mater. 3 (2004) 539-544.

[30] Q. Huang, D. Jiang, I.A. Ovid'Ko, A. Mukherjee, High-current-induced damage on carbon nanotubes: The case during spark plasma sintering, Scr. Mater. 63 (2010) 1181-1184.

[31] E.L. Corral, H. Wang, J. Garay, Z. Munir, E.V. Barrera, Effect of single-walled carbon nanotubes on thermal and electrical properties of silicon nitride processed using spark plasma sintering, J. Eur. Ceram. Soc. 31 (2011) 391-400.

[32] E. Ermer, P. Wiesław, S. Ludosław, Influence of sintering activators on structure of silicon carbide, Sol. Stat. Ion. 141-142 (2001) 523-528.

[33] M. Balog, P. Šajgalík, M. Hnatko, Z. Lencéš, F. Monteverde, J. Keckéš, J.L. Huang, Nano-versus macro-hardness of liquid phase sintered SiC, J. Eur. Ceram. Soc. 25 (2005) 529-534.

[34] B. Bhushan, Introduction to tribology. John Wiley & Sons, Inc., 2002.

[35] H. Czichos, D. Klaffke, E. Santner, M. Woydt, Advances in tribology: the materials point of view, Wear 190 (1995) 155-161.

[36] G. Yamamoto, T. Hashida, K. Adachi, T. Takagj, Tribological Properties of Single-Walled Carbon Nanotube Solids, J. Nanosci. Nanotechnol. 8 (2008) 2665-2670.

[37] M.S. Suh, Y.H. Chae, S.S. Kim, Friction and wear behavior of structural ceramics sliding against zirconia, Wear 264 (2008) 800-806.

Figure captions:

Figure 1. First-order micro-Raman spectra for the CNFs starting powders and CNFs material after treatment by SPS at different temperatures. D/G intensity ratios are depicted on right corner.

Figure 2. Relative density of monolithic, Al_2O_3/CNFs and SiC/CNFs composites fabricated by SPS technique at 1500 ºC and 1600 ºC, respectively.

Figure 3. Hardness of ceramic-CNFs composites as a function of CNFs content.

Figure 4. Wear rate of monolithic ceramics, CNFs and ceramic-CNFs composites in function of CNFs content.

Figure 5. The friction coefficient of Al_2O_3, SiC, CNFs and ceramic-CNFs composites as a function of CNFs contents (left) and distance (right).

Figure 6 SEM micrographs of damaged surface after the wear tests; (a) Al_2O_3/CNFs (80/20), (b) Al_2O_3/CNFs (20/80), (c) SiC/CNFs (80/20) and (d) SiC/CNFs (20/80) vol.%.

Figure 1

Click here to download high resolution image

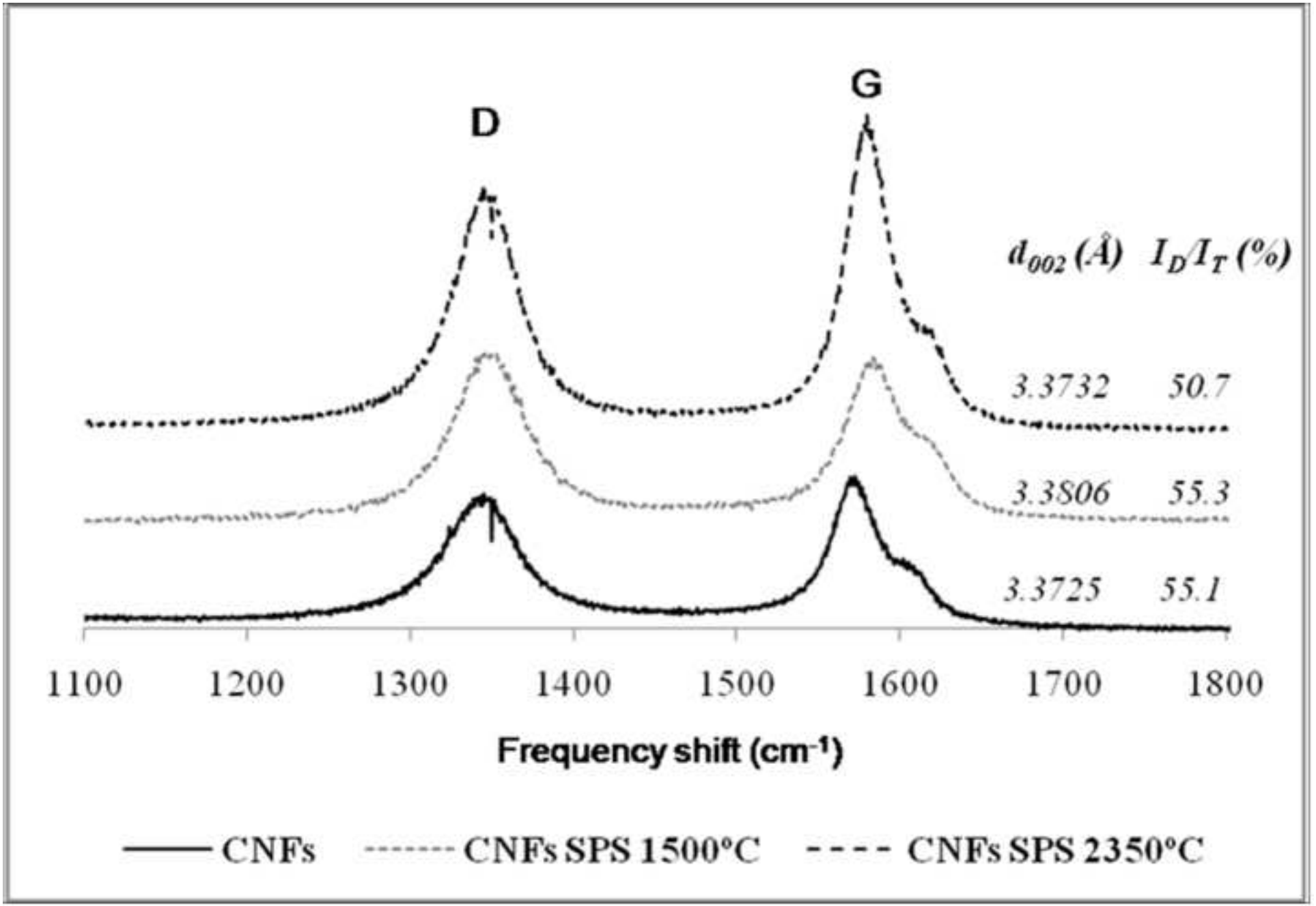

Figure 2
Click here to download high resolution image

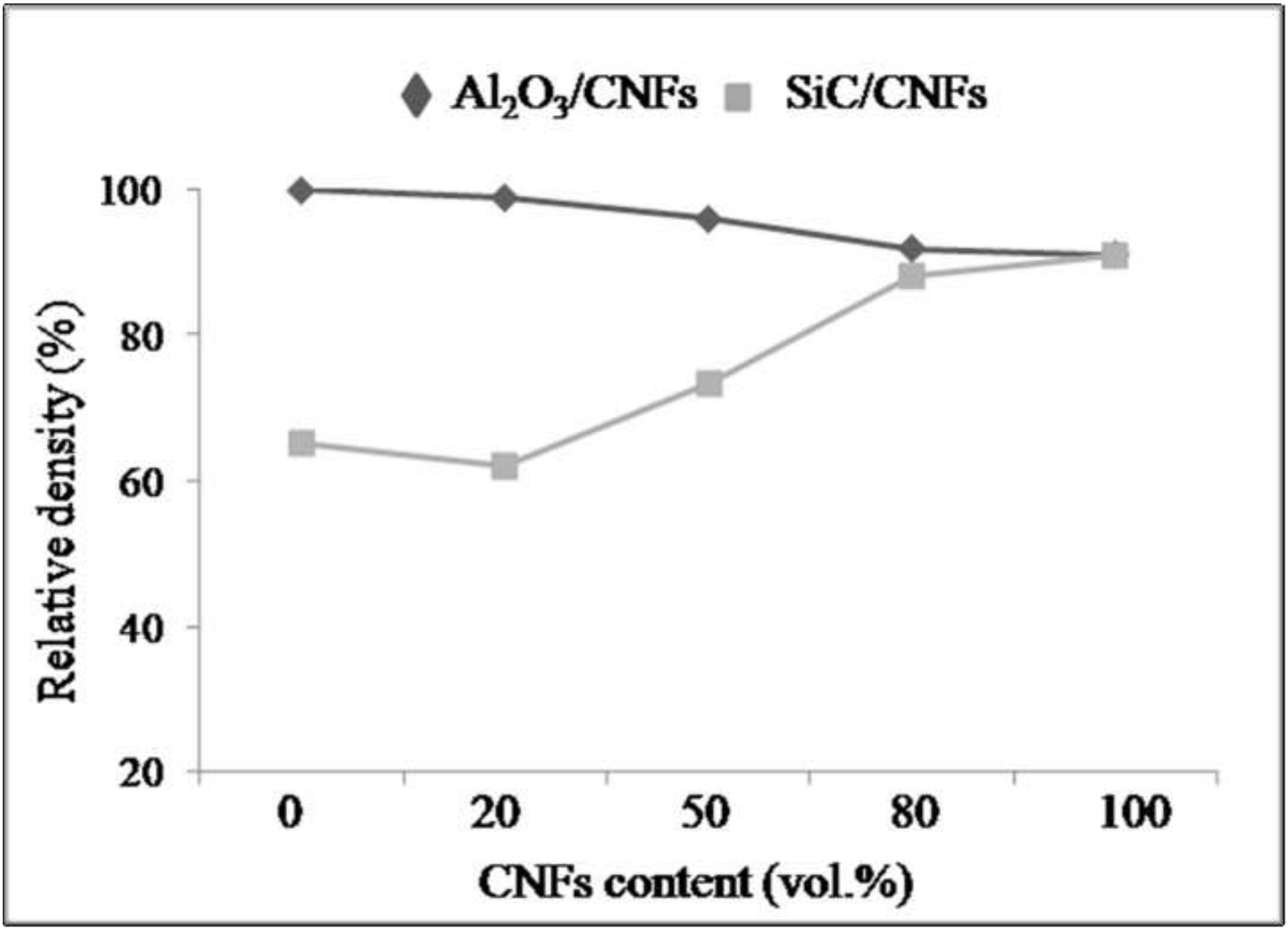

Figure 3
Click here to download high resolution image

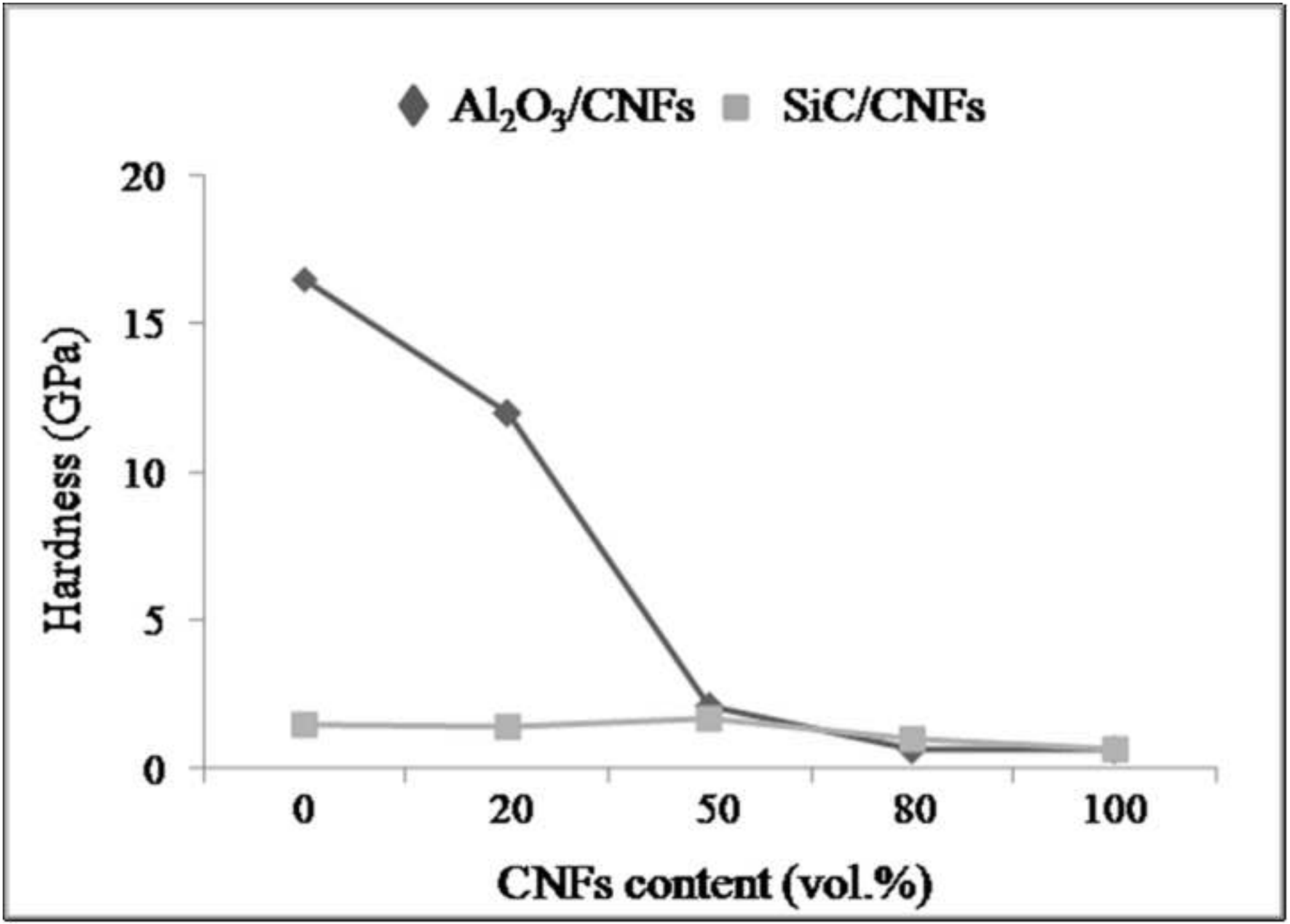

Figure 4

Click here to download high resolution image

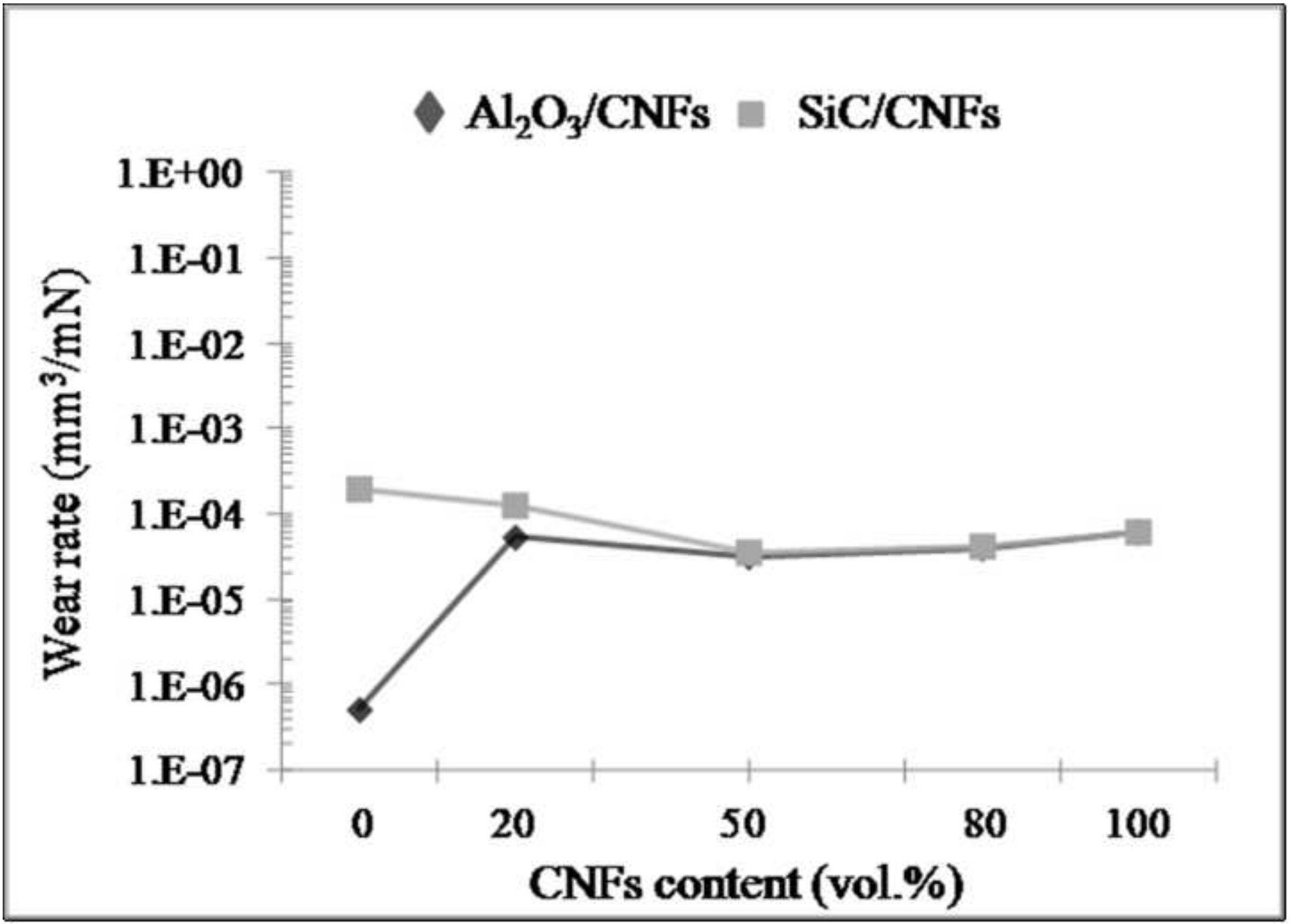

Figure 5

Click here to download high resolution image

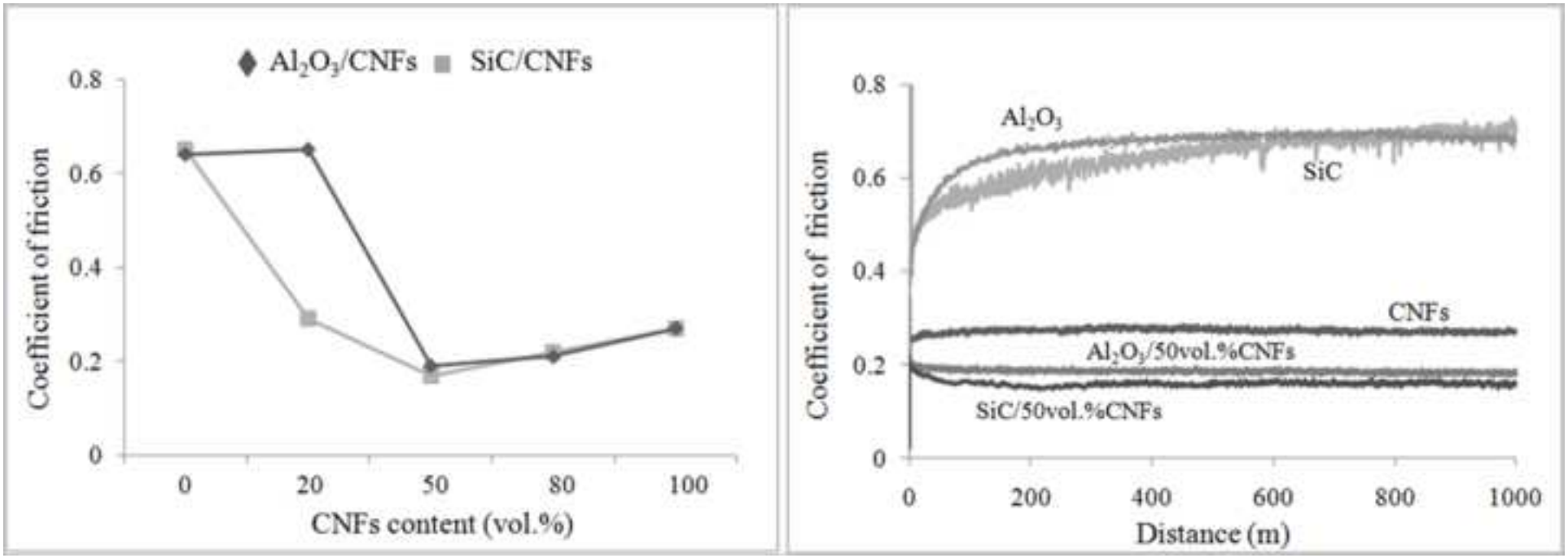

Figure 6

Click here to download high resolution image